Mikailalsys Journal of
Advanced Engineering International
e-ISSN : 3046-9694
p-ISSN : 3046-8914
Index : Harvard, Boston, Sydney University, Dimensions, Lens, Scilit, Semantic, Google, etc
https://doi.org/10.58578/MJAEI.v3i1.8180

Impact of Periodic Body Acceleration on Fractional Blood Flow Modeled as a Non-Newtonian Jeffery-Type Fluid in Stenosed Arteries

Shehu Adamu Aliyu & Habujika Abdulhadi Ismail
Bill and Melinda Gates College of Health Technology Ningi, Bauchi State Nigeria
Federal University Wukari, Taraba State, Nigeria
isahabdullahi7474@gmail.com

Article Info:

Submitted:	Revised:	Accepted:	Published:
Dec 10, 2025	Jan 25, 2026	Feb 11, 2026	Feb 16, 2026

Abstract

This study comprehensively explores the impact of hemodynamic parameters on nanoparticle transport and blood flow dynamics in stenosed arteries, with the objective of identifying how these parameters can be manipulated to improve targeted drug delivery and circulatory function in regions affected by vascular constriction. A mathematical model was formulated that incorporates externally induced factors, including baseline blood flow rates, the pulsatile nature of cardiac-induced oscillations, phase angles between these oscillations and the flow, and externally applied periodic body acceleration (PBA). The analysis reveals that increasing baseline blood flow enhances the distribution of oxygen and nutrients throughout the arterial system, highlighting the importance of optimized base flow conditions for maintaining tissue perfusion in stenotic regions. The incorporation of pulsatile flow characteristics that mimic natural heartbeat-induced oscillations leads to improved shear stress distribution along arterial walls, which may help prevent plaque formation and reduce the

MJAEI Journal is licensed under a Creative Commons Attribution-NonCommercial-ShareAlike 4.0 International License

progression of arterial narrowing. Variations in phase angle, representing the temporal shift between flow oscillations and external stimuli, were shown to influence the synchronization between blood flow and externally applied forces, with consequent effects on hemodynamic efficiency and the timing of flow responses in stenosed vessels. Furthermore, the introduction of PBA substantially increases nanoparticle mobility within the bloodstream, reducing the likelihood of particle stagnation in low-flow regions and enhancing the efficiency of nanoparticle-based drug delivery. Overall, the findings underscore the potential of optimizing fluid dynamic parameters and employing PBA as a non-invasive strategy to augment drug perfusion and support vascular health, providing a theoretical basis for the development of more effective targeted cardiovascular therapies and motivating future translational studies to assess clinical feasibility and therapeutic efficacy.

Keywords: Periodic Body Acceleration; Non-Newtonian Jeffery-Type Fluid; Fractional Model; Stenosed Arteries; Nanoparticle Velocity Profile.

INTRODUCTION

Over the past several decades, the study of blood flow dynamics has attracted significant attention across diverse scientific and engineering disciplines due to the realization that blood is not a Newtonian fluid. Instead, it exhibits a set of highly complex rheological behaviors that make its analysis both intriguing and challenging. Blood's non-Newtonian properties stem from its unique composition and the interactions between its various constituents. These properties include shear-thinning behavior (where viscosity decreases with increased shear rate), viscoelasticity (exhibiting both fluid-like and solid-like responses), and thixotropy (where viscosity changes over time under constant shear) [1]. Such behaviors are critical to understanding the physiological processes governing blood flow, particularly under varying hemodynamic conditions such as pulsatile flow, bifurcations, or high-shear stress in narrowed vessels. Blood is the essential life-sustaining fluid in the human body, and it performs multiple vital roles. It is primarily responsible for the **transport of oxygen from the lungs to tissues, the distribution of nutrients absorbed from the digestive system, the removal of metabolic waste products such as carbon dioxide and urea, and the circulation of hormones and immune cells that help regulate body function and defend against infection. The biophysical behavior of blood within arteries, veins, and capillaries directly affects the efficiency and health of these functions. Consequently, accurate modeling of blood flow is

not just an academic pursuit but a critical component of clinical diagnostics, therapeutic planning, and biomedical engineering.

The composition of blood significantly contributes to its non-Newtonian nature. It consists of approximately 55% plasma, which is largely water but also includes dissolved proteins (such as albumin and fibrinogen), glucose, clotting factors, and electrolytes. The remaining 45% of blood volume is composed of cellular components, primarily red blood cells (erythrocytes), along with white blood cells (leukocytes) and platelets (thrombocytes). Among these, red blood cells dominate in both volume and influence on viscosity. They possess flexible membranes that allow deformation as they pass through narrow capillaries and contribute significantly to shear-thinning behavior. Furthermore, red blood cells carry a negative surface charge, which influences their electrostatic interactions with the walls of arteries and other cells. These interactions can generate a localized magnetic field, especially in curved or stenotic arteries, where disturbed flow and wall interactions are pronounced. This electromagnetic influence has been shown to impact flow dynamics and can play a role in magnetohydrodynamic modeling of blood flow [3]. The simulation and analysis of hemodynamic behavior through mathematical modeling and numerical simulation have become indispensable in both research and clinical contexts. The capability to simulate how blood behaves in healthy and diseased states has enabled significant advancements in our understanding and treatment of conditions such as atherosclerosis (plaque buildup in arteries), aneurysms (ballooning of arterial walls), stenosis (narrowing of blood vessels), and vascular remodeling. These conditions are among the leading causes of cardiovascular disease, which remains one of the top causes of death globally [2]. Through computational models, clinicians can predict areas of high shear stress, identify regions vulnerable to plaque formation, and optimize the design of medical devices like stents, catheters, and artificial valves.

To accurately represent the nonlinear and memory-dependent behavior of blood, researchers have increasingly turned to fractional calculus, a branch of mathematical analysis that extends the concept of derivatives and integrals to non-integer orders. Unlike traditional (integer-order) calculus, fractional calculus offers a more flexible and precise framework for describing the hereditary and time-dependent characteristics of complex fluids. In biological systems, where current states often depend on past interactions and deformation histories, fractional models provide a better fit for observed behaviors and experimental data [4]. This has led to the formulation of fractional differential equations (FDEs) in hemodynamics,

capable of capturing the subtleties of blood flow with improved accuracy. Within the wide range of models available to represent non-Newtonian fluids, the Jeffrey model stands out as one of the most extensively used for representing viscoelastic materials. This model is particularly effective in capturing both relaxation (how stress decays under constant strain) and retardation (the delayed response to applied stress), which are essential for understanding how blood behaves under dynamic flow conditions. The model incorporates two-time constants one for relaxation and another for retardation providing a more comprehensive depiction of fluid behavior than simpler models like the Maxwell or Newtonian frameworks. Recent advancements have seen the Jeffrey model extended using fractional derivatives, resulting in the fractional Jeffrey model, which has been shown to align closely with experimental results and is especially useful in analyzing blood flow under pulsatile and oscillatory conditions [5].

Therefore, the transition from classical to fractional non-Newtonian models in blood flow dynamics marks a significant step forward in our ability to simulate and interpret complex biological fluids. These models not only account for the non-Newtonian nature of blood but also reflect its viscoelastic, electromagnetic, and time-dependent properties more accurately than ever before. This evolution in modeling methodology has far-reaching implications in medical diagnostics, surgical planning, and the design of biomedical devices, offering the potential for more personalized and precise interventions in cardiovascular medicine.

Fractional calculus has emerged as a powerful and versatile mathematical tool for modeling a wide range of physical phenomena, especially those involving memory effects and hereditary properties, which are intrinsic to many biological and engineering systems. In the context of blood flow dynamics, fractional derivatives provide a more comprehensive and flexible modeling framework compared to traditional classical methods, which are often restricted to local and instantaneous descriptions of system behavior. The nonlocal nature of fractional derivatives makes them particularly well-suited for capturing the complex viscoelastic and time-dependent properties of blood, which cannot be fully addressed using conventional integer-order differential models. Over the past decade, researchers have increasingly turned their attention to external physical influences such as magnetic fields, electric fields, and magnetic nanoparticles, especially due to their relevance in medical applications like targeted drug delivery, hyperthermia treatment, and magnetic resonance imaging (MRI) [6]. These studies have shown that the inclusion of electromagnetic forces in

blood flow models significantly alters flow profiles, shear stress distributions, and heat transfer rates within the vascular system. Despite this progress, the majority of previous investigations in this area have been confined to classical fluid models, particularly Jeffrey-type fluids, which assume non-fractional, time-independent rheological properties. In particular, the studies presented in [7] focused on the non-fractional Jeffrey fluid model, examining how it behaves under different external influences. While these models have been instrumental in understanding certain aspects of blood flow, they fall short in terms of capturing the long-term memory effects and history-dependent behaviors of blood an important limitation given that blood exhibits both elastic and viscous characteristics that are inherently time-dependent. Moreover, the research in [8] acknowledged the influence of electric fields on blood flow but did not investigate these effects within the context of a fractional framework, thus leaving an important dimension of the problem unaddressed.

Meanwhile, more recent developments in the literature, such as the works of [9] and [10], have extended the scope of fractional modeling by applying fractional-order derivatives to Maxwell and Burger's fluids, thereby offering improved predictive capabilities for complex fluid flows. These models have provided deeper insights into relaxation and retardation phenomena, which are critical in viscoelastic materials. Nevertheless, despite these advancements, there remains a notable gap in research regarding the combined effects of electric fields and fractional viscoelasticity in the Jeffrey fluid model, which continues to be one of the most relevant and widely used models for describing biological fluids like blood. As pointed out in [11], this oversight has limited our understanding of how electromagnetic and mechanical forces simultaneously influence fractional blood flow, particularly in conditions simulating real physiological environments.

To bridge this important research gap, the present study proposes a novel extension of the classical Jeffrey fluid model by integrating fractional-order time derivatives along with the inclusion of electric field effects and periodic body acceleration (PBA). Periodic body acceleration, which can occur due to muscular activity, respiration, or external motion, plays a significant role in altering flow characteristics in living organisms. By incorporating PBA, the model becomes more representative of in vivo conditions, particularly in situations involving forced oscillations or time-varying gravitational environments, such as during physical exercise, in vehicular motion, or in aerospace applications. Furthermore, the inclusion of electromagnetic forces, particularly electric fields, is crucial for modeling the behavior of blood a conducting ionic fluid—within the cardiovascular system. Electric fields

can arise naturally due to ion transport, or they can be externally applied during medical procedures. Their interaction with charged components of blood, especially negatively charged red blood cells, significantly affects flow dynamics. When these electric fields are considered in conjunction with fractional viscoelasticity, it becomes possible to capture a richer and more nuanced picture of the electro-hemodynamic environment of the human body.

Therefore, the current study provides a comprehensive and generalized framework that not only builds on existing classical models but also significantly advances the field by capturing the interplay between periodic mechanical acceleration, fractional-order memory effects, and electromagnetic forces. This approach allows for the simulation of more realistic and physiologically accurate blood flow scenarios, offering enhanced insight into various biomedical applications. The resulting model is expected to be a valuable tool for researchers and practitioners working in biomechanics, cardiovascular fluid dynamics, and biomedical engineering, particularly in areas related to noninvasive diagnostics, targeted drug delivery, and the design of medical devices such as pumps, stents, and sensors for smart health systems.

MODELING OF THE PROBLEM

Schematic diagram of the problem

This investigation centers on the hemodynamic behavior of blood flow, specifically under conditions where the flow is incompressible, pulsatile, laminar, and axisymmetric—an idealized yet physiologically relevant scenario representative of blood movement through small- to medium-sized arteries. These vessels are typically characterized by a low shear rate, which is a key factor influencing the rheological behavior of blood. Under such conditions, the non-Newtonian properties of blood become particularly prominent due to the aggregation and deformation of red blood cells and their interaction with plasma. To accurately capture this complex flow behavior, the study adopts the Jeffrey fluid model, a well-established non-Newtonian framework that accounts for both viscous and elastic effects by incorporating relaxation and retardation times.

In addition to modeling blood as a Jeffrey fluid, the analysis integrates the influence of magnetic nanoparticles, which are increasingly used in biomedical applications such as magnetic drug targeting, hyperthermia treatment, and diagnostic imaging. These particles,

when suspended in blood, interact with externally applied magnetic fields, thereby modifying the flow characteristics. Their inclusion adds a layer of complexity to the model while enhancing its applicability to modern therapeutic and diagnostic techniques.

The study is carried out within a cylindrical segment of an artery of finite length L, providing a geometrically appropriate representation of a vascular channel. The flow is described using a cylindrical coordinate system (r, θ, z), which allows the analysis of fluid motion in three orthogonal directions: axial (z-direction, along the length of the artery), radial (r-direction, outward from the central axis), and azimuthal (θ-direction, around the circumference of the vessel). This coordinate framework not only aligns with the anatomical structure of arteries but also simplifies the governing equations under the assumption of axisymmetric flow, where variables are independent of the azimuthal angle. By focusing on this controlled yet physiologically pertinent setup, the investigation seeks to elucidate the effects of non-Newtonian viscoelasticity, magnetic nanoparticle interaction, and pulsatile flow on the overall blood dynamics within confined vascular domains. The findings are anticipated to provide valuable insights into both normal circulatory function and pathological conditions, while also contributing to the optimization of nanoparticle-based therapies and medical device design.

Figure 1 illustrates the geometry of a non-tapered stenosed artery modeled with varying shape parameters m = 2, 4, and 8. The figure depicts how the shape parameter m influences the severity and sharpness of the stenosis within the arterial segment. When m = 2, the stenosis exhibits a relatively smooth and gradual constriction, representing a mild narrowing of the artery. As the value of m increases to 4 and then to 8, the shape of the stenosis becomes increasingly sharper and more severe, indicating a more abrupt and pronounced narrowing. This variation in the shape parameter allows for a comparative analysis of different stenotic geometries and their potential impact on blood flow dynamics within the artery.

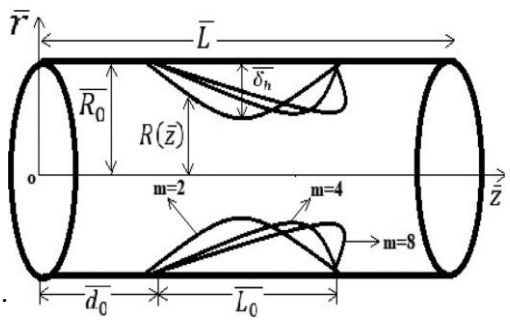


Figure 1: Geometry of the Non-Tapered Stenosed Artery with Different Shape Parameter m = 2,4 and 8

The governing equations for the proposed physical model are constructed by integrating principles from fluid dynamics, non-Newtonian rheology, and electromagnetism, thereby forming a comprehensive framework for analyzing pulsatile blood flow in the presence of magnetic influences and nanoparticle suspensions. At the core of this formulation lies the Navier–Stokes equations, which govern the conservation of linear momentum and mass in fluid systems. These equations describe how the velocity field of the blood evolves over time under the influence of internal stresses, pressure gradients, and external body forces.

To accurately represent the non-Newtonian characteristics of blood, particularly under low shear conditions, the classical Navier–Stokes model is augmented with the Jeffrey constitutive equation. This model captures both viscous and elastic responses of blood flow by introducing two-time constants: the relaxation time, which measures the delay in stress response to deformation, and the retardation time, which describes the delay in strain relative to stress. As a result, the Jeffrey fluid model is well-suited for representing blood's viscoelastic and shear-thinning behavior in arterial flow conditions. In addition to fluid mechanical forces, the model incorporates electromagnetic effects, which arise due to the application of an external transverse magnetic field. The interaction between the magnetic field and the electrically conducting blood generates Lorentz forces, which act to resist the flow and alter the velocity profile. These electromagnetic interactions are mathematically described by Maxwell's equations and Ohm's law, which relate the induced currents and magnetic fields to the fluid motion and applied electromagnetic parameters. In the presence of magnetic nanoparticles, the magnetic susceptibility of the fluid is further modified, leading to enhanced magneto-hydrodynamic (MHD) effects. The full system of governing equations is therefore composed of:

$$\nabla \bullet \overline{B_0} = 0, \nabla \times \overline{B_0} = \overline{\mu_0}\overline{J}, \nabla \times \overline{E} = -\frac{\partial \overline{B_0}}{\partial \bar{t}} \qquad (1)$$

where $\overline{B_0}$ and $\overline{E}$ define the respective flux intensities for both the magnetic and electric fields respectively.

$\overline{J}$ represents the current density, derivable from the generalized Ohm's law as follows

$$\overline{J} = \overline{\sigma}\left(\overline{E} + \overline{V} + \overline{B_0}\right), \qquad (2)$$

where $\overline{V}$ and $\overline{\sigma}$ are the flow velocity field and the electric conductivity respectively.

The resultant electromagnetic body force acting on the on the blood is given by:

$$\overline{F}_{emf} = \overline{\rho_e}\,\overline{E} + \overline{J} \times \overline{B_0} = \overline{\rho_e}\,\overline{E} + \overline{\sigma}\left(\overline{E} + \overline{V} + \overline{B_0}\right) \times \overline{B_0} \qquad (3)$$

where $\overline{u}_f, \overline{\rho}_e$ and $\overline{E}_z$ are the axial fluid velocity, the free electric charge density, and the axial component of the externally applied electric field are denoted respectively. Accordingly, the net electromagnetic body force acting on the fluid accounted for in the momentum equation is given by

$$\overline{F}_{emf} = \overline{\rho_e}\,\overline{E_z} - \overline{\sigma}\,\overline{B}_0^{\,2}\,\overline{u}_f \qquad (4)$$

Basic Flow Equations

The movement of any fluid is governed by the fundamental law of mass conservation, which ensures that mass is neither created nor destroyed within a flow system. In the realm of fluid mechanics, this physical law is described mathematically through the continuity equation. This equation implies that the amount of mass entering a given region must precisely balance the amount leaving, after considering any changes in mass stored within that region over time. In the context of time-dependent (unsteady) flow behavior of a Jeffrey-type non-Newtonian fluid characterized by both viscous and elastic properties this conservation principle, along with Newton's second law applied to fluid motion, leads to the formulation of the continuity and momentum equations in differential form as presented below:

$$\left.\begin{aligned}-\overline{\rho}\left[\frac{\partial}{\partial \overline{t}}+\overline{v}_f\frac{\partial}{\partial \overline{r}}+\overline{u}_f\frac{\partial}{\partial \overline{z}}\right]\overline{v}_f=-\frac{\partial \overline{P}}{\partial \overline{r}}+\\ \frac{1}{\overline{r}}\frac{\partial}{\partial \overline{r}}\left(\overline{r}\,\overline{S}_{\overline{r}\overline{r}}f\right)+\frac{\partial}{\partial \overline{z}}\left(\overline{S}_{\overline{r}\overline{z}}f\right)-\frac{\overline{S}_{\overline{\theta}\overline{\theta}f}}{\overline{r}}\end{aligned}\right\} \tag{5}$$

$$\left.\begin{aligned}-\overline{\rho}\left[\frac{\partial}{\partial \overline{t}}+\overline{v}_f\frac{\partial}{\partial \overline{r}}+\overline{u}_f\frac{\partial}{\partial \overline{z}}\right]\overline{u}_f=-\frac{\partial \overline{P}}{\partial \overline{z}}+\\ \frac{1}{\overline{r}}\frac{\partial}{\partial \overline{r}}\left(\overline{r}\,\overline{S}_{\overline{z}\overline{r}}f\right)+\frac{\partial}{\partial \overline{z}}\left(\overline{S}_{\overline{z}\overline{z}}f\right)+\overline{\rho}_e\overline{E}_{\overline{z}}\\ -\overline{\sigma}\overline{B}_0^2\overline{u}+\overline{K}_s\overline{N}_p\left(\overline{u}_p-\overline{u}_f\right)+\overline{G}\left(\overline{t}\right)\end{aligned}\right\} \tag{6}$$

$$\frac{\partial \overline{v}_f}{\partial \overline{r}}+\frac{\overline{v}_f}{\overline{r}}+\frac{\partial \overline{u}_f}{\partial \overline{z}}=0 \tag{7}$$

And the extra stress tensors of Jeffrey fluid are given by:

$$\left.\begin{aligned}\overline{S}_{\overline{r}\overline{r}}f&=\frac{2\overline{\mu}}{1+\lambda_1}\left[1+\overline{\lambda}_2\left(\overline{v}_f\frac{\partial}{\partial \overline{r}}+\overline{u}_f\frac{\partial}{\partial \overline{z}}\right)\right]\frac{\partial \overline{v}_f}{\partial \overline{r}}\\ \overline{S}_{\overline{r}\overline{z}}&=\overline{S}_{\overline{z}\overline{r}}=\frac{\overline{\mu}}{1+\lambda_1}\left[1+\overline{\lambda}_2\left(\overline{v}_f\frac{\partial}{\partial \overline{r}}+\overline{u}_f\frac{\partial}{\partial \overline{z}}\right)\right]\\ &\left(\frac{\partial \overline{v}_f}{\partial \overline{z}}+\frac{\partial \overline{u}_f}{\partial \overline{r}}\right)\\ \overline{S}_{\overline{\theta}\overline{\vartheta}}f&=\frac{2\overline{\mu}}{1+\lambda_1}\left[1+\overline{\lambda}_2\left(\overline{v}_f\frac{\partial}{\partial \overline{r}}+\overline{u}_f\frac{\partial}{\partial \overline{z}}\right)\right]\frac{\overline{v}_f}{\overline{r}}\\ \overline{S}_{\overline{z}\overline{z}}f&=\frac{2\overline{\mu}}{1+\lambda_1}\left[1+\overline{\lambda}_2\left(\overline{v}_f\frac{\partial}{\partial \overline{r}}+\overline{u}_f\frac{\partial}{\partial \overline{z}}\right)\right]\frac{\partial \overline{u}_f}{\partial \overline{z}}\end{aligned}\right\} \tag{8}$$

where $\overline{u}_f$ and $\overline{v}_f$ denote the fluid velocity components in the axial and radial direction, $\overline{\rho}_e$ is the density of the fluid suspension, $\overline{P}$ is the pressure, λ_1 and $\overline{\lambda}_2$ are the relaxation and retardation time respectively, $\overline{B}_0$, the applied uniform magnetic field, $\overline{\mu}$ is the dynamic viscosity of the fluid, $\overline{K}_s$ is the Stokes constant, $\overline{N}_p$ is the quantity of magnetic nanoparticles in each unit volume of blood and $\frac{\overline{K}_s\overline{N}_p\left(\overline{u}_p-\overline{u}_f\right)}{\rho}$

is the force exerted due to the interaction between the movement of particles and the fluid. and $\overline{G}\left(\bar{t}\right)$ is the periodic body force.

Then the momentum equation governing the flow of fluid in the cylindrical coordinate system is given by [12,13,14,15,16,17,18,19 20]:

$$\left.\begin{aligned}\overline{\rho}\frac{\partial \bar{u}_f}{\partial \bar{t}} = \frac{\partial \overline{P}}{\partial \bar{z}} + \frac{\overline{\mu}}{1+\lambda_1}\left[\frac{1}{\bar{r}}\frac{\partial}{\partial \bar{r}}\left(\bar{r}\frac{\partial \bar{u}}{\partial \bar{r}}\right)\right] + \\ \overline{K}_s \overline{N}_p\left(\bar{u}_p - \bar{u}_f\right) + \overline{\rho}_e \overline{E}_{\bar{z}} - \overline{\sigma}\overline{B}_0^2 \bar{u} + \overline{G}\left(\bar{t}\right)\end{aligned}\right\} \qquad (9a)$$

and a_0, a_1 are the amplitude of steady pulsatile component of pressure gradient respectively and $\overline{\omega}_p = 2\pi \overline{f}_p . \overline{f}_p$ is the frequency of pulse.

where

$$G(\bar{t}) = \overline{A}\ \cos(\bar{k}\bar{t} + \Phi_0) \qquad (9b)$$

is the periodic body acceleration.

Assuming that the nanoparticles possess an effective hydrodynamic radius, are homogeneously dispersed throughout the fluid medium, and are transported in unison with the surrounding fluid, their motion is influenced by multiple interacting forces. These include the magnetic force arising from the applied magnetic field, the buoyant force due to density differences between the particles and the fluid, and the drag or fluidic force exerted by the moving fluid. The combined effect of these forces governs the dynamics of the nanoparticles, leading to the formulation of the momentum equation in the axial direction, which can be expressed as:

$$\overline{M}_p \frac{\partial \bar{u}_p}{\partial \bar{z}} = \sum \overline{F}_{tex} \qquad (10)$$

where

$\sum \overline{F}_{tex}$ Is the**total force** acting on the nanoparticles is generally the combined effect of magnetic, buoyancy, and fluidic (drag) forces. However, by neglecting the influence of buoyancy and assuming that the particles are solely subjected to the drag force exerted by the surrounding fluid, the motion of the particles can be described using Stokes's law [21, 22].

Under this assumption, the governing equation for particle flow simplifies accordingly and is given as:

$$\overline{M}_p \frac{\partial \bar{u}_p}{\partial \bar{z}} = \overline{K}_s \left(\bar{u}_f - \bar{u}_p \right) \tag{11}$$

where $\overline{M}_p$ is the mass of single particle, $\bar{u}_p - \bar{u}_f$ is the relative velocity and $\overline{K}_s = 6\pi \overline{\mu} \overline{E}_{hyd.p} \left(\bar{u}_f - \bar{u}_p \right)$ is the Stokes constant and the negative sign indicate that the motion of the fluid and particles are in opposite directions.

The corresponding initial and boundary conditions are for the proposed problem as:

$$\bar{u}\left(\bar{r},0\right) = 0, \frac{\partial \bar{u}\left(\bar{r},0\right)}{\partial \bar{t}} = 0, \bar{u}\left(1,\bar{t}\right) = 0 \tag{12}$$

With the aid of electrostatics theory, the relationship between the net charge $\overline{\rho}_e$ and the electric field $\overline{\psi}\left(\bar{r}\right)$ can be described using Coulomb's law and the principle of superposition. The net charge refers to the total amount of electric charge within a system, which can be either positive or negative. This charge creates an electric field that influences other charges in the vicinity.

$$\left.\begin{aligned} \nabla^2 \overline{\psi}\left(\bar{r}\right) = \frac{1}{\bar{r}} \frac{\partial}{\partial \bar{r}} \left(\bar{r} \frac{\partial \overline{\psi}\left(\bar{r}\right)}{\partial \bar{r}} \right) + \\ \frac{1}{\bar{r}^2} \frac{\partial^2 \overline{\psi}\left(\bar{r}\right)}{\partial \bar{z}} = \frac{\overline{\rho}_e\left(\bar{r}\right)}{\in} \end{aligned}\right\} \tag{13}$$

Known as the Boltzmann equation with the boundary condition and the net charge density

$$\overline{\psi}(1) = \overline{\psi}_w \text{ and } \frac{\partial \overline{\psi}}{\partial \bar{r}} = 0, \text{ at } \bar{r} = 0 \tag{14}$$

$$\overline{\rho}_e\left(\bar{r}\right) = e_0\left(n^+ - n^-\right) = \frac{-2z_0^2 e_0^2 n_0 \overline{\psi}\left(\bar{r}\right)}{k_g T_e} \tag{15}$$

where $\in$ is the dielectric constant, $\overline{\psi}_w$ is the potential on the arterial wall, $z_0, n_0, e_0, k_g, T_e, n^+$ and n^- are the ion valence, concentration of ions, the electronic charge,

the Boltzmann constant, the local absolute temperature of the fluid, the density number of cations and anions respectively.

UsingDebye-Huckel parameter

$$\bar{k}^2 = \frac{2z_0^2 e_0^2 n_0 \bar{\psi}(\bar{r})}{\in k_g T_e}$$

and linearized the Boltzmann equation we get a potential equation as:

$$\frac{1}{\bar{r}} \frac{\partial}{\partial \bar{r}} \left(\bar{r} \frac{\partial \bar{\psi}(\bar{r})}{\partial \bar{r}} \right) = \bar{k}^2 \bar{\psi}(\bar{r}) \tag{16}$$

The introducing dimensionless parameter to the flow governing equations are:

$$\left.\begin{aligned} {}_f = \frac{\bar{u}_f}{u_0}, u_p = \frac{\bar{u}_p}{u_0}, r = \frac{\bar{r}}{R_0}, z = \frac{\bar{z}}{R_0}, \\ u t = \bar{\omega}_p \bar{t}, P = \frac{\bar{P} R_0^2}{\mu u_0}, a_0 = \frac{\bar{a}_0 R_0}{\mu u_0}, a_1 = \frac{\bar{a}_1 R_0^2}{\mu u_0} \\ S = \frac{\bar{S} R_0^2}{\mu u_0}, \psi = \frac{\bar{\psi}}{\bar{\psi}_w}, A_0 = \frac{R_0 \bar{A}_0}{u_0} \end{aligned}\right\} \tag{17}$$

Applying equation (17) to equations (9)-(11) and (16) subject to the dimensionless initial and boundary conditions and dropping the bars yield to the following equations:

$$\frac{1}{r} \frac{\partial}{\partial r} \left(r \frac{\partial \psi(r)}{\partial r} \right) - K_e^2 \psi(r) = 0 \tag{18}$$

$$\left.\begin{aligned} \beta^2 \frac{\partial u_f}{\partial t} = -\frac{\partial P}{\partial z} + \frac{1}{1+\lambda_1} \left[\frac{1}{r} \frac{\partial}{\partial r} \left(r \frac{\partial u_f}{\partial r} \right) \right] + \\ A_0 \cos(kt + \phi) + R_c (u_p - u_f) - M^2 u_f + \\ K^2 \psi(r) \end{aligned}\right\} \tag{19}$$

$$\beta^2 G \frac{\partial u_p}{\partial t} = u_f - u_p \tag{20}$$

$$\psi(1)=1,\frac{\partial\psi(0)}{\partial r}=0,u(r,0)=0,\\ \frac{\partial u(r,0)}{\partial t}=0,u(1,t)=0 \tag{21}$$

where

$$\beta^2=\frac{\overline{\omega}_p\overline{\rho}R_0^2}{\mu},R_c=\frac{\overline{K}_s\overline{N}_pR_0^2}{\mu},\\ G=\frac{\overline{M}_p\mu}{\overline{\rho}R_0^2\overline{K}_s},M^2=\frac{\overline{\sigma}\overline{B}_0^2R_0^2}{\mu}$$

and $K_e^2=\overline{k}^2R_0^2$ are the oscillatory Reynolds number (Womersley parameter), particle density parameter, Hartmann number (magnetic field parameter), and electrokinetic breadth parameter.

Solution Techniques

The solution to equation (18) subject to equation (21) is

$$\psi(r)=\frac{I_0(K_er)}{I_0(K)} \tag{22}$$

where I_0 is the modified Bessel function of first kind and order zero.

To more accurately represent the inherent memory effects and intricate temporal behavior of the fluid flow, we adopt a time-fractional formulation of the momentum equations. These equations are constructed using the Caputo–Fabrizio fractional derivative, which features a non-singular kernel and is particularly effective in modeling systems with fading memory and complex relaxation characteristics.

$$\left.\begin{aligned} &{}^{CF}D_t^{\alpha}u(r,t)=\frac{1}{1-\alpha}\int_0^t\frac{\partial u(r,\tau)}{\partial\tau}exo\\ &\left(-\frac{\alpha(t-\tau)}{1-\alpha}\right)d\tau,0<\alpha<1\\ &L\left\{{}^{CF}D_t^{\alpha}u(r,t)\right\}=\frac{su(r,s)-u(r,0)}{(1-\alpha)s+\alpha} \end{aligned}\right\} \tag{23}$$

The fractional differential equation, which includes the Caputo-Fabrizio fractional derivative, is now established to represent the momentum equations (18–20), accounting for

the intricate flow dynamics and memory effects within the system.The Caputo–Fabrizio (CF) derivative offers several advantages over classical fractional models like the Caputo derivative, particularly in modeling physical and biological systems. One of the main advantages is that the CF derivative uses a non-singular and exponential kernel, in contrast to the singular power-law kernel used in the Caputo derivative. This leads to smoother and more realistic modeling of memory effects in physical systems without the mathematical complexity introduced by singularities. Additionally, the CF derivative is better suited for problems with finite memory, making it more practical for simulating real-world phenomena where long-term memory is not dominant. It also ensures well-posed initial conditions similar to classical derivatives, allowing easier interpretation and implementation in initial value problems.

$$\begin{aligned}&\beta^{2\,CF}D_t^{\alpha}u_f(r,t)=f(t)+\\&\frac{1}{1+\lambda_1}\left[\frac{1}{r}\frac{\partial}{\partial r}\left(r\frac{\partial u_f(r,t)}{\partial r}\right)\right]\\&+R_c\left(u_p(r,t)-u_f(r,t)\right)\\&-M^2u_f(r,t)-K^2\psi(r)\end{aligned}\quad . \tag{24}$$

$$\beta^2 G^{CF}D_t^{\alpha}u_p(r,t)=u_f(r,t)-u_p(r,t) \tag{25}$$

where

$$\begin{aligned}f(t)&=-\frac{\partial\overline{P}}{\partial\overline{z}}+G(t)\\&=a_0+a_1\cos(\omega t)+A_0\cos(kt+\phi)\end{aligned} \tag{26}$$

Applying Laplace transform on equations (25) and (26), and using the definition in equation (23) we have:

$$\left.\begin{aligned}&\beta^2\frac{su_f(r,s)-u(r,0)}{(1-\alpha)s+\alpha}=F(s)+\\&\frac{1}{1+\lambda_1}\left[\frac{1}{r}\frac{\partial}{\partial r}\left(r\frac{\partial u_f(r,s)}{\partial r}\right)\right]+\\&R_c\left(u_p(r,s)-u_f(r,s)\right)\\&-M^2u_f(r,s)-\frac{K^2}{s}\psi(r)\end{aligned}\right\} \tag{27}$$

$$\beta^2 \frac{su_p(r,s)-u(r,0)}{(1-\alpha)s+\alpha} = u_f(r,s)-u_p(r,s) \quad (28)$$

where $u_f(r,s)=\int_0^\infty u_f(r,t)e^{-st}dt, u_p(r,s)=\int_0^\infty u_p(r,t)e^{-st}dt$

and

$$F(s)=\int_0^\infty f(t)e^{-st}dt$$

$K^2\psi(r)$ is a constant with respect to time t.

Rearranging equations (27) and (28)

$$\begin{aligned}&\beta^2 \frac{su_f(r,s)}{(1-\alpha)s+\alpha} = F(s)+\\ &\frac{1}{1+\lambda_1}\left[\frac{1}{r}\frac{\partial}{\partial r}\left(r\frac{\partial u_f(r,s)}{\partial r}\right)\right]+\\ &R_c\left(u_p(r,s)-u_f(r,s)\right)\\ &-M^2u_f(r,s)-\frac{K^2}{s}\psi(r)\end{aligned} \quad (29)$$

$$\beta^2 G\frac{su_p(r,s)}{(1-\alpha)s+\alpha} = u_p(r,s)-u_f(r,s) \quad (30)$$

Making $u_p(r,s)$ subject in equation (30) and substitute in equation (31), and rearranging we have

$$u_p(r,s)=\left[\frac{(1-\alpha)s+\alpha}{\beta^2 Gs+(1-\alpha)s+\alpha}\right]u_f(r,s) \quad (31)$$

$$\begin{aligned}&\left[\frac{\beta^2 s+R_c\beta^2 Gs+M^2\left[(1-\alpha)s+\alpha\right]}{(1-\alpha)s+\alpha}\right]u_f(r,s)\\ &=F(s)+\frac{1}{1+\lambda_1}\left[\frac{1}{r}\frac{\partial}{\partial r}\left(r\frac{\partial u_f(r,s)}{\partial r}\right)\right]\\ &-\frac{K^2}{s}\psi(r)\end{aligned} \quad (32)$$

Applying the finite Henkel transform of order zero to equation (34), we obtained

$$\left[\frac{\beta^2 s + R_c\beta^2 Gs + M^2\left[(1-\alpha)s+\alpha\right]}{(1-\alpha)s+\alpha}\right]u_f(\gamma_n,s)$$
$$= F(s)\frac{J_1(\gamma_n)}{\gamma_n} + \frac{1}{1+\lambda_1}\left[\gamma_n^2 u_f(\gamma_n,s)\right] \quad (33)$$
$$-\frac{K^2}{s}\frac{\gamma_n}{\gamma_n^2+K^2}J_1(\gamma_n)$$

$$u_f(\gamma_n,s) = \left[\frac{\left[(1-\alpha)s+\alpha\right](1+\lambda_1)}{Q(s)}\right]$$
$$\left[F(s)\frac{J_1(\gamma_n)}{\gamma_n} - \frac{K^2}{s}\frac{\gamma_n}{\gamma_n^2+K^2}J_1(\gamma_n)\right] \quad (34)$$

$$Q(s) = a_n s + b_n\alpha$$
$$a_n = \beta^2(1+\lambda_1)(1+R_cG)+$$
$$M^2(1+\lambda_1)(1-\alpha)+\gamma_n^2(1-\alpha)$$
$$b_n = M^2(1+\lambda_1)+\gamma_n^2 \quad (35)$$
$$F(s) = \frac{a_0}{s} + \frac{a_1 s}{s^2+\omega^2} +$$
$$A_0\left(\frac{s\cos\phi - k\sin\phi}{k^2+s^2}\right)$$

Now applying the inverse Henkel transform on equation (34) we have

$$u_f(r,s) = \left[\frac{\left[(1-\alpha)s+\alpha\right](1+\lambda_1)}{Q(s)}\right]$$
$$\left[F(s)\Omega(r) - \frac{1}{s}\Phi(r)\right] \quad (36)$$

where

$$\Omega(r) = 2\sum_{n=1}^{\infty}\frac{J_0(\gamma_n r)}{\gamma_n J_1(\gamma_n)}$$

and

$$\Phi(r) = 2\sum_{n=1}^{\infty}\frac{K^2\gamma_n}{\gamma_n^2+K^2}\frac{J_0(\gamma_n r)}{J_1(\gamma_n)}$$

And for the velocity of the magnetic nanoparticles, we substitute equation (36) into equation (31) and obtained

$$u_p(r,s) = \left[\frac{(1-\alpha)s+\alpha}{\beta^2 Gs+(1-\alpha)s+\alpha}\right] \left[\frac{[(1-\alpha)s+\alpha](1+\lambda_1)}{Q(s)}\right] \left[F(s)\Omega(r)-\frac{1}{s}\Phi(r)\right] \quad (37)$$

The inverse Laplace transformofEquations (36)–(37) was determined using Gerby-Stephan's Algorithm, and the results were graphically simulated with the aid of MATHCAD software.

RESULTS AND DISCUSSION

This study focused on the fractional modeling of blood flow through stenosed arteries using a Jeffrey-type non-Newtonian fluid under the influence of periodic body acceleration (PBA), electric, and magnetic fields. The results revealed notable interactions between the flow dynamics and key hemodynamic parameters, offering valuable insights for medical and therapeutic applications.In this regard, we assume the following dimensionless physical parameters suchas$a_0 = 0.5, a_1 = 0.5, \omega_p = \frac{\pi}{4}. G = 0.8, \lambda_1 = 0.4, M = 1.0, K = 0.5, A0 = 0.5, R = 0.5,\ \beta = 0.7.$

Nomenclature Table

Symbol	Description	Unit
r, z, θ	Radial, axial, and azimuthal coordinates in cylindrical system	m (meters), rad
u, v	Axial and radial velocity components	m/s
P	Density of blood or suspension fluid	kg/m³
P	Pressure	Pa
M	Dynamic viscosity of the fluid	Pa·s
λ_1	Relaxation time (Jeffrey fluid)	S
λ_2	Retardation time (Jeffrey fluid)	S
Σ	Electrical conductivity of blood	S/m
B_0	Strength of applied magnetic field	T
E_0	Applied electric field strength	V/m

Symbol	Description	Unit
ϱ_e	Free electric charge density	C/m^3
J	Electric current density	A/m^2
Φ	Electric potential	V
E	Dielectric constant of the fluid	F/m
z_i	Valence of ion species i	Dimensionless
E	Elementary charge	C
kB	Boltzmann constant	J/K
T	Absolute temperature	K
n_i	Ion number density	$ions/m^3$
Np	Number of magnetic nanoparticles per unit volume	$particles/m^3$
Fm	Magnetic body force	N
Fd	Drag force on nanoparticles	N
Mp	Mass of single magnetic nanoparticle	Kg
B	Stokes drag coefficient	kg/s
Vr	Relative velocity between fluid and particles	m/s
A	Amplitude of pulsatile pressure gradient	Pa/m
Ω	Frequency of oscillation	rad/s
L	Length of artery segment	M
R	Radius of artery	M
M	Shape parameter of the stenosis	Dimensionless
A	Womersley number (oscillatory Reynolds number)	Dimensionless
Ha	Hartmann number (magnetic field parameter)	Dimensionless
Sc	Schmidt number (momentum vs. mass diffusivity)	Dimensionless
Re	Reynolds number	Dimensionless
λD	Debye length	M
K	Debye–Hückel parameter	1/m
$\bar{u}, \bar{r}, \bar{z}$	Dimensionless velocity, radial and axial coordinates	Dimensionless
Ψ	Dimensionless electric potential	Dimensionless

Velocity Field Profile

The results from Figures 2–5 show that increasing the baseline blood flow and oscillatory amplitude significantly improves velocity distribution and overall flow efficiency. This aligns with the findings of Akbar et al. [23], who emphasized the role of enhanced baseline flow in improving perfusion, especially in compromised arteries. Moreover, the observed enhancement in pulsatile behavior is consistent with the Womersley effect, which suggests that pulsatile flow modulates shear stress, potentially reducing arterial plaque buildup [24]. The impact of phase shifts on velocity synchronization further indicates that hemodynamic delays could be managed through phase-tuned oscillatory interventionsa concept supported by previous work on phase-sensitive flow dynamics in cardiovascular systems [25].

The results reinforce the utility of PBA as a non-invasive tool to improve circulation. As seen in Figures 5 and 6, PBA effectively reduces stagnation zones and enhances nanoparticle transport. This complements earlier reports which demonstrated that external mechanical stimulation, such as whole-body vibration or PBA, can augment microcirculatory dynamics and vascular compliance [26, 27].

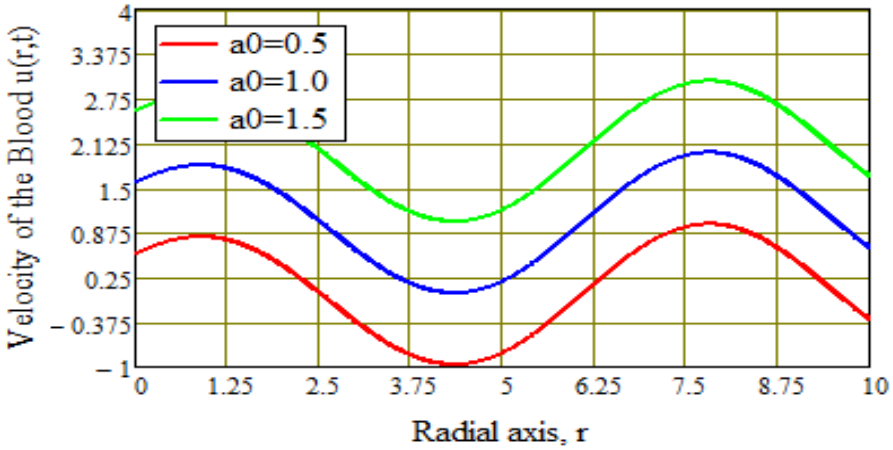


Figure 2: Variation of dimensionless fluid velocity with radial distance for different values of Baseline blood flow/pressurea0

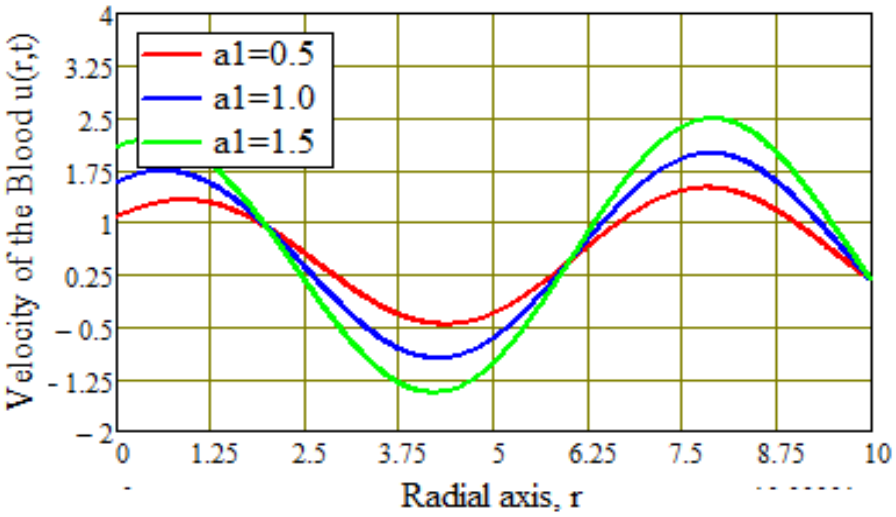


Figure 3: Variation of dimensionless fluid velocity with radial distance for different values of the amplitude of heartbeat-induced oscillations, a1

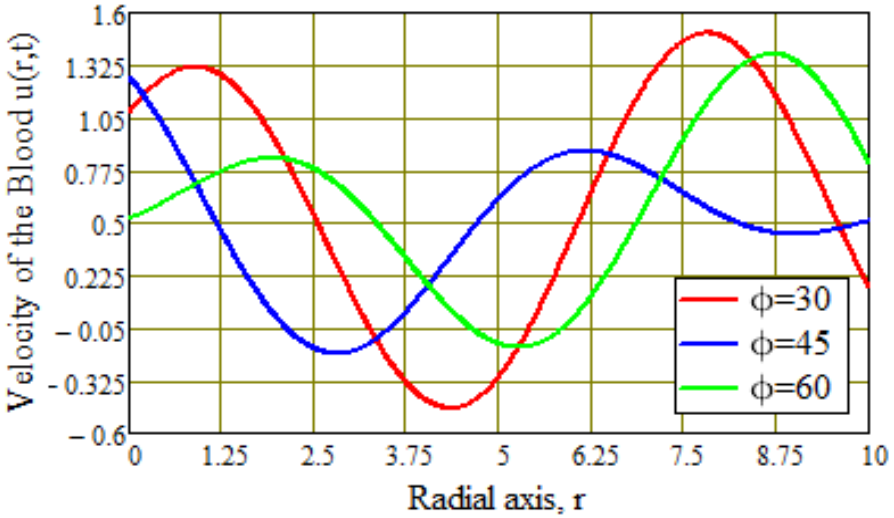


Figure 4: Variation of dimensionless fluid velocity with radial distance for different values of the phase angle.

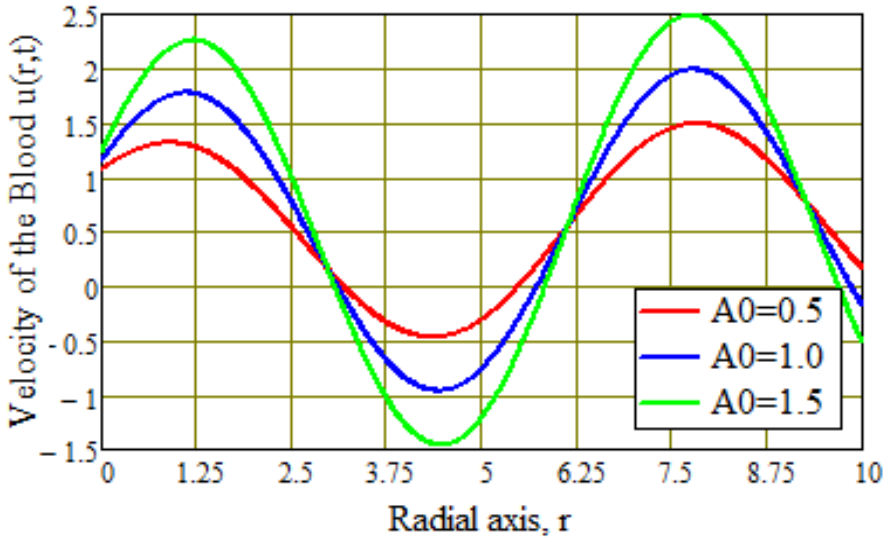


Figure 5: *Dimensionless Fluid velocity distribution with radial distance for different values Scaling factor for external oscillations,A0*

Figure 2 illustrates that an increase in the baseline blood flow parameter leads to a higher velocity distribution across the radial distance. This is attributed to the steady component of blood flow, which contributes to the overall momentum of the fluid and ensures the continuous transport of oxygen and nutrients. Physiologically, this effect mirrors the mean arterial pressure (MAP), which plays a crucial role in regulating blood perfusion to various organs. **Figure 3** demonstrates that higher values of the blood flow parameter result in more pronounced oscillatory behavior in blood velocity. This is expected, as the parameter represents the amplitude of periodic fluctuations induced by the cardiac cycle. When this value is high, the oscillations become more prominent, simulating conditions of increased heart rate or external mechanical influences (e.g., exercise). These results are consistent with the influence of the Womersley parameter, which suggests that pulsatile flow enhances shear stress distribution, thereby reducing the likelihood of arterial blockages. **Figure 4** shows the impact of phase shifts on the synchronization of blood velocity with imposed periodic acceleration. A shift in phase alters the timing of peak velocity, which may influence hemodynamic delays in cases of arterial stenosis. The findings imply that phase delays in pulsatile blood flow could lead to delayed perfusion, particularly affecting organs that rely on real-time blood delivery, such as the brain and kidneys. **Figure 5** highlights that an increase in the blood flow parameter significantly affects velocity distribution. The externally imposed oscillations, such as those from whole-body vibration therapy, enhance blood movement and may help reduce stagnation effects near the arterial walls. These results

suggest the potential clinical application of periodic body acceleration (PBA) to improve blood circulation, especially in areas with stenosed arteries.

Nanoparticle Velocity Profile

Figures 6–9 extend the findings to magnetic nanoparticles (MNPs), showing that their motion is closely tied to changes in flow parameters, including oscillatory amplitude and phase angle. These findings resonate with recent developments in magnetically guided drug delivery systems, where time-dependent modulation of the flow field is used to optimize nanoparticle dispersion and target-site delivery [28]. The use of fractional models with memory effects (via Caputo–Fabrizio derivatives) enhances the predictive accuracy of nanoparticle behavior under physiological conditions, supporting studies by Ionescu et al. [29] that stress the role of fractional calculus in modeling biological complexity.

Since the study also considers magnetic nanoparticles (MNPs) suspended in the bloodstream, their velocity distributions were analyzed under similar parametric variations.

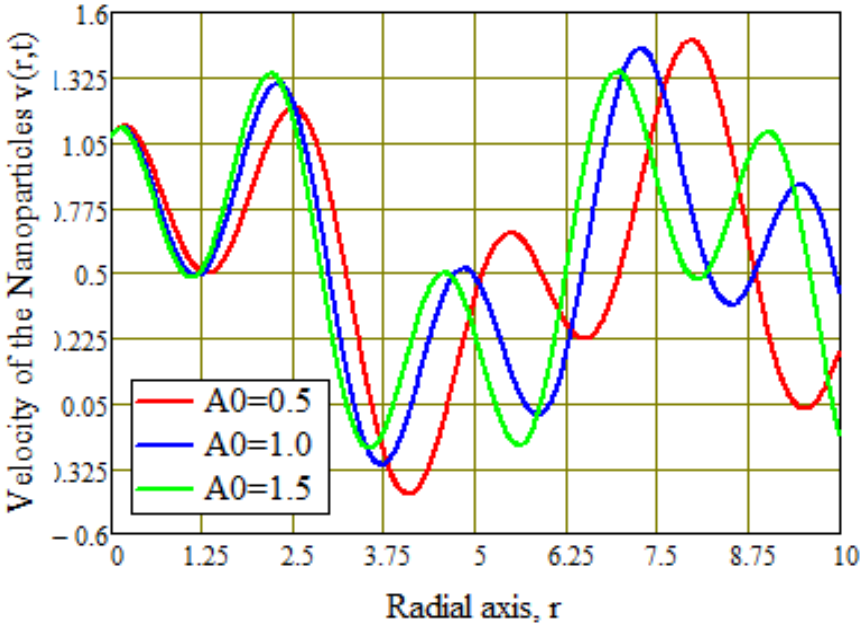


Figure 6: Variation of dimensionless nanoparticle velocity with radial distance for different values of the scaling factor for external oscillations,A0

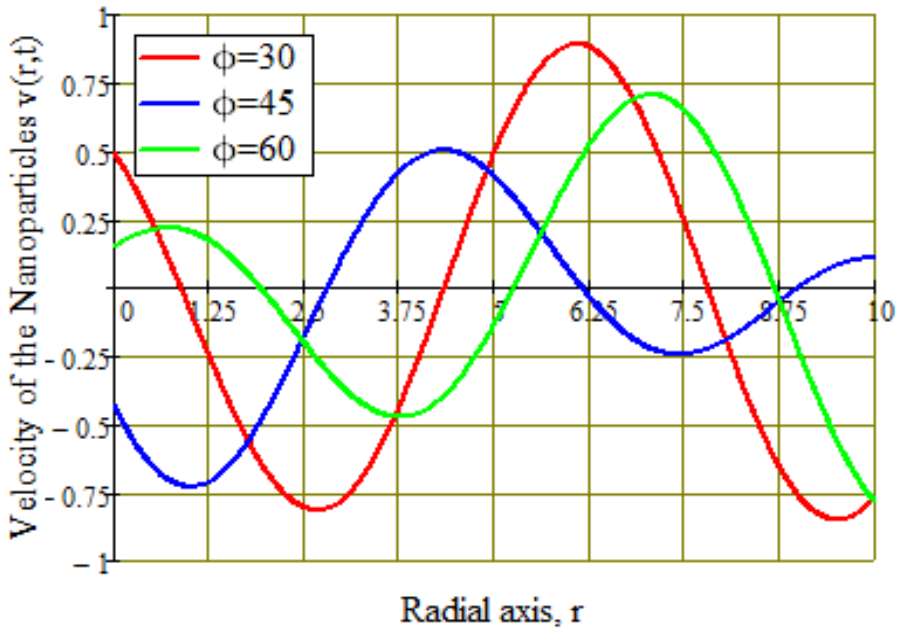


Figure 7: Dimensionless Nanoparticle velocity distribution with radial distance for different values of Phase angle

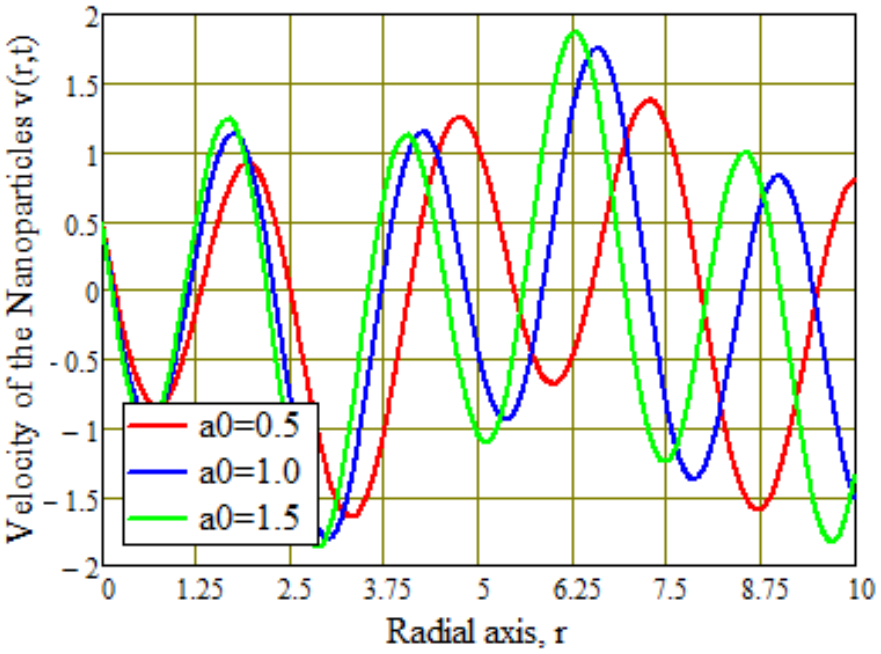


Figure 8: Dimensionless Nanoparticle velocity distribution with radial distance for different values of Baseline blood flow/pressure, a0

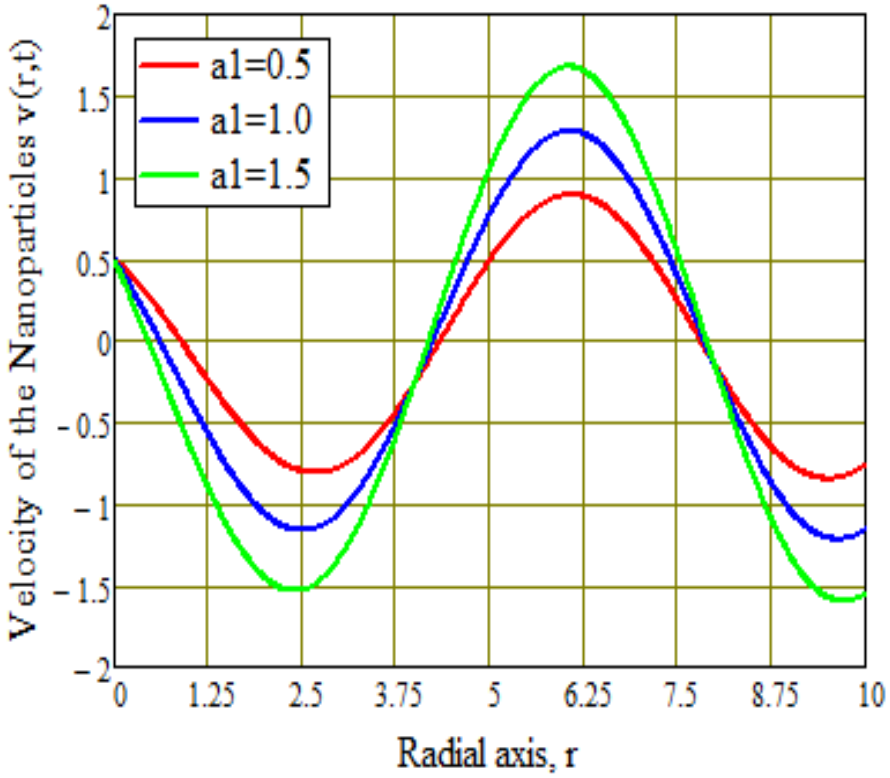


Figure 9: Dimensionless Nanoparticle velocity distribution with radial distance for different values of Amplitude of heartbeat-induced oscillations, a1 **Figure 6** shows that increasing PBA enhances nanoparticle motion, suggesting that PBA improves nanoparticle transport. This increase in mobility is significant for targeted drug delivery applications, as it suggests that PBA can effectively enhance nanoparticle movement, facilitating drug perfusion in stenosed arteries. **Figure 7** demonstrates that phase shifts influence nanoparticle velocity in a manner similar to that of bulk blood velocity. This finding highlights the importance of time-dependent oscillations in controlling nanoparticle delivery, which is valuable for the design of efficient magnetically guided drug therapies. By optimizing phase-controlled nanoparticle release, drug delivery systems can be better tailored. **Figures 8 and 9** reveal the roles of both parameters in regulating nanoparticle motion. Higher values lead to a more uniform flow of nanoparticles, while higher values induce pulsatile variations. These pulsatile changes can be utilized for controlled drug release mechanisms, providing potential advantages in therapeutic applications.

Broader Implications and Future Directions

These findings collectively suggest that oscillatory flow mechanicsespecially those influenced by PBAcould be leveraged in cardiovascular interventions. Specifically, optimized timing and scaling of oscillations might improve perfusion in ischemic tissues and facilitate controlled drug dispersion in targeted therapies. Future studies should investigate the applicability of these findings in patient-specific geometries and under more physiologically variable conditions. Further experimental validation, particularly with in vivo models or clinical trials incorporating external mechanical stimulation, will also help translate these theoretical insights into practice [29,30].

CONCLUSION

This study investigated the influence of various hemodynamic parameters on nanoparticle transport and blood flow dynamics, with a particular focus on their implications for targeted drug delivery and circulation improvement in stenosed arteries. The findings reveal that increasing the baseline blood flow parameter enhances velocity distribution, ensuring continuous oxygen and nutrient transport, which is critical for maintaining proper organ perfusion. Additionally, higher oscillatory behavior in blood velocity, influenced by periodic cardiac fluctuations, contributes to enhanced shear stress distribution, potentially mitigating arterial blockages.

The study further demonstrates that phase shifts in pulsatile blood flow affect the synchronization of blood velocity with imposed periodic acceleration, which could have clinical significance in managing hemodynamic delays associated with arterial stenosis. Moreover, the results indicate that externally imposed oscillations, such as periodic body acceleration (PBA), significantly improve blood circulation by enhancing nanoparticle mobility and reducing stagnation effects near arterial walls. This suggests a promising application of PBA in therapeutic interventions aimed at improving drug perfusion in compromised vascular regions.

Funding: Not Applicable.

Acknowledgments: Our sincere appreciations go to the referees for their contributions in making this article successful.

Conflict of interest: The authors declare no conflict of interest.

REFERENCES

[1] Abdulhameed, M., Vieru, D., & Roslan, R. (2017). Modelling electro-magneto-hydrodynamic transport of biofluids with a new trend of fractional derivative without singular kernel. *Physica A: Statistical Mechanics and Its Applications*.

[2] Abdulhameed, M., Roslan, R., & Mohamad, M. B. (2014). A modified homotopy perturbation transform method for transient flow of a third-grade fluid in a channel with oscillating motion on the upper wall. *Journal of Computational Engineering*, 2014, Article 102197, 1–11.

[3] Akbar, S., Nadeem, S., & Ali, M. (2011). Jeffrey fluid model for blood flow through a tapered artery with a stenosis. *Journal of Mechanics in Medicine and Biology*, *11*, 529–545.

[4] Mahapatra, T. R., & Pradhan, B. C. (2022). Effects of chemical reactions on nanofluid flows in biological systems. *Advances in Fluid Mechanics*, *57*(3), 178–195.

[5] Singh, R., & Kumar, D. (2023). Heat and mass transfer enhancement in ternary nanofluid flows: Influence of Dufour and Soret effects. *Scientific Reports*, *11*(9).

[6] Zhao, L. F., et al. (2022). Entropy analysis and heat transfer characteristics of Casson nanofluid flow in inclined arteries. *Physica A: Statistical Mechanics and Its Applications*, *605*.

[7] Mondal, A., & Shit, G. C. (2017). Transport of magneto-nanoparticles during electro-osmotic flow in a micro-tube in the presence of magnetic field for drug delivery application. *Journal of Magnetism and Magnetic Materials*, *442*, 319–328.

[8] Anand, M., Aggarwal, S., Raj, H., & Gajjar, D. (2023). CFD analysis of pulsatile non-Newtonian blood flow in a multi-staged stenosed bifurcated carotid artery. *J. Mines, Met. Fuels*, *71*(10), 1601–1611.

[9] Akhtar, S., McCash, L. B., Nadeem, S., Saleem, S., & Issakhov, A. (2021). Mechanics of non-Newtonian blood flow in an artery having multiple stenosis and electroosmotic effects. *Science Progress*, *104*(3), 1–20.

[10] Sankar, D. S., & Lee, U. (2022). Numerical study on pulsatile flow of non-Newtonian fluid through arterial stenosis. *Journal of Mechanical Science and Technology*, *36*(3), 1235–1244.

[11] Chakravarty, S., & Mandal, P. K. (2022). Augmentation of peristaltic microflows through electro-osmotic mechanisms. *Journal of Physics D: Applied Physics*, *55*(12), Article 125401.

[12] Ghasemi, S. E., Hatami, M., Sarokolaie, A. K., & Ganji, D. D. (2022). Study on blood flow containing nanoparticles through porous arteries in presence of magnetic field using analytical methods. *Physica E: Low-dimensional Systems and Nanostructures*, *135*, Article 114984.

[13] Selim, M. M., & Mohamed, E. M. (2023). Heat and mass transfer in peristaltic transport of non-Newtonian fluid through porous medium with slip and magnetic effects. *Alexandria Engineering Journal*, *69*, 631–645.

[14] Rao, K. S., & Kumar, R. S. (2022). Fractional modeling of nanofluid flow through an irregular artery with multiple stenoses. *Mathematics*, *10*(21), Article 4082.

[15] Ijaz, M., Ahmad, H., Rauf, A., & Khan, M. I. (2023). Hemodynamic analysis of non-Newtonian nanofluid flow through arterial stenosis under magnetic field effects. *Case Studies in Thermal Engineering*, *43*, Article 102750.

[16] Farooq, M., Gul, M., & Ali, N. (2023). Comparative study of blood flow in tapered and non-tapered arteries under different non-Newtonian models. *Alexandria Engineering Journal*, *72*, 179–193.

[17] Ullah, I., Khan, I., & Qureshi, M. I. (2022). Dynamics of non-Newtonian blood flow with chemical reaction and heat source/sink in an inclined artery with stenosis. *Journal of Thermal Analysis and Calorimetry*, *148*, 4161–4175.

[18] Sadiq, M. A., & Shah, N. A. (2023). Numerical investigation of hybrid nanofluid in a stenosed artery considering radiative effects. *Results in Physics*, *47*, Article 106322.

[19] Yakubu, D. G., Abdulhameed, M., Adamu, G. T., & Kwami, A. M. (2020). A study of fractional relaxation time derivative on blood flow in arteries with magnetic and thermal radiation effects. *Jour. Eng. Fluid Flow and Heat Trans. Analysis*, *26*, 126–144.

[20] Yakubu, D. G., Abdulhameed, M., Adamu, G. T., Rozaini, R., Alibek, I., Rahimi-Gorji, M., & Bakouri, M. (2021). Towards the exact solution of Burgers' fluid flow through arteries with fractional time derivative, magnetic field, and thermal radiation effects. *Proceedings of the Institution of Mechanical Engineers, Part E: Journal of Process Mechanical Engineering*, 1–10.

[21] Hayat, M., Waqas, S., Shahzad, A., & Alsaedi, A. (2015). MHD stagnation point flow of Jeffrey fluid by a radially stretching surface with viscous dissipation and joule heating. *Journal of Hydrology and Hydromechanics*, *63*, 311–317.

[22] Ionescu, C., Lopes, A., Copot, D., Machado, J. A. T., & Bates, J. H. T. (2017). The role of fractional calculus in modeling biological phenomena: A review. *Communications in Nonlinear Science and Numerical Simulation*.

[23] Sun, Y., Fan, Y., & Deng, X. (2014). Computational study of pulsatile blood flow in arteries with different degrees of stenosis. *Computers in Biology and Medicine*, *53*, 27–36.

[24] Bertram, C. D., & Macaskill, C. (2011). Phase relationships in oscillatory blood flow: Importance in pulsatile modeling. *Journal of Biomechanics*, *44*(4), 684–691.

[25] Cardinale, M., & Bosco, C. (2003). The use of vibration as an exercise intervention. *European Journal of Applied Physiology*, *90*(3–4), 347–352.

[26] Maloney-Hinds, C., Petrofsky, J. S., & Zimmerman, G. (2008). The effect of 30 Hz vs. 50 Hz passive vibration and duration of vibration on skin blood flow in the arm. *Medical Science Monitor*, *14*(3), CR112–CR116.

[27] Arya, M., et al. (2008). Controlled magnetic nanoparticle delivery using external magnetic fields for targeted therapy. *Nanomedicine*, *3*(6), 667–675.

[28] Magin, R. L. (2010). *Fractional calculus in bioengineering*. Begell House Publishers.

[29] Tzeng, T. R., & Tsai, C. (2015). Magnetically driven nanoparticles for targeted drug delivery systems. *Journal of Biomedical Nanotechnology*, *11*(10), 1720–1733.

[30] Ibrahim, A., & Ahmed, M. (2021). Mechanically assisted perfusion techniques for vascular therapy: A systematic review. *Cardiovascular Therapeutic*